ChemComm

Chemical Communications

www.rsc.org/chemcomm

Number 2 | 14 January 2008 | Pages 125–264

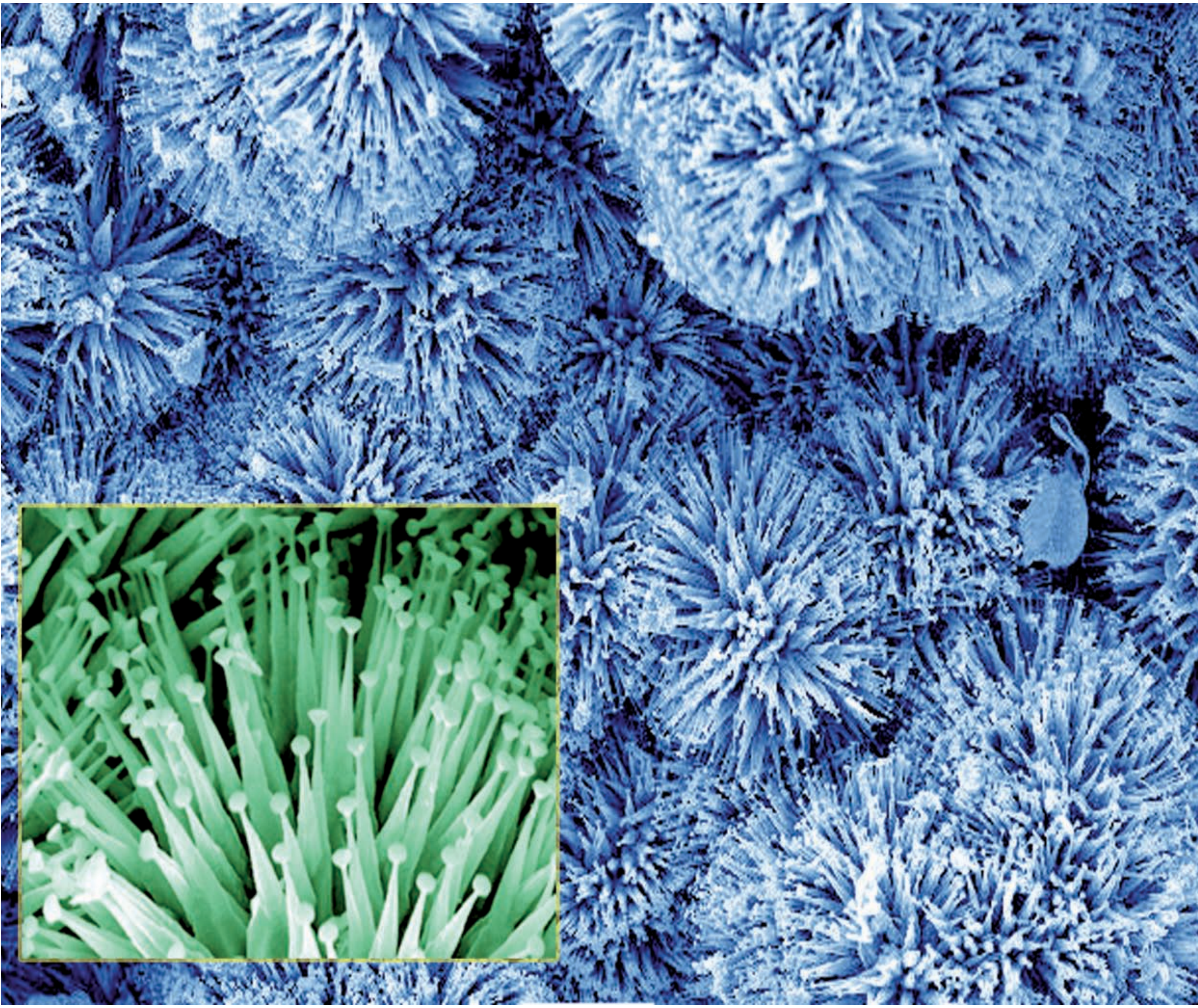

ISSN 1359-7345

COMMUNICATION

Ahmad Umar, Mohammed Muzibur Rahman, Sang Hoon Kim and Yoon-Bong Hahn

Zinc oxide nanonail based chemical sensor for hydrazine detection

FEATURE ARTICLES

James F. Rusling *et al.*

Biochemical applications of ultrathin films of enzymes, polyions and DNA

Ulrich S. Schubert *et al.*

Asymmetrical supramolecular interactions

RSC Publishing

1359-7345(2008)2;1-5

COMMUNICATION www.rsc.org/chemcomm | ChemComm

Zinc oxide nanonail based chemical sensor for hydrazine detection†

Ahmad Umar, Mohammed Muzibur Rahman, Sang Hoon Kim and Yoon-Bong Hahn*

Received (in Cambridge, UK) 23rd July 2007, Accepted 28th September 2007
First published as an Advance Article on the web 17th October 2007
DOI: 10.1039/b711215g

Using ZnO nanonails, a hydrazine electrochemical sensor has been fabricated, for the first time, which showed a high and reproducible sensitivity of 8.56 μA cm^{-2} μM^{-1} with a response time less than 5 s, a linear range from 0.1 to 1.2 μM and a correlation coefficient of R = 0.999. The limit of detection (LOD), based on the S/N ratio, was estimated to be 0.2 μM.

Hydrazine is widely used as a fuel in rocket propulsion systems and has a low threshold limit value (TLV) of 10 ppb.[1] It is also used in missile systems, fuel cells, pesticides, photography chemicals, weapons for mass destruction, catalysts, emulsifiers, dyes, corrosion inhibitors, and so on.[2–4] It is a neurotoxin, and hence produces carcinogenic and mutagenic effects causing damage to lungs, liver, and kidneys, respiratory tract infection and long-term effects on the central nervous system.[5,6] Due to the aforesaid reasons, it is highly desirable to fabricate a reliable and sensitive analytical tool for the effective detection of hydrazine. For that purpose, electrochemical techniques offer an opportunity for portable, cheap and rapid methodologies. A variety of chemically modified electrodes, based on different electrocatalytic moieties (electron-mediator species), have thus been developed for the detection of hydrazine which include the metal complexes of phthalocyanine,[7] porphyrins,[8,9] hexacyanoferrates,[10,11] Nafion/ruthenium(III),[12] and a few others.[13–15] Moreover, due to the exotic properties of nanostructures, some researchers have also demonstrated the use of carbon nanotubes as electron mediators, to modify the electrodes for the detection of hydrazine.[16–18] Having exotic and versatile properties including biocompatibility, nontoxicity, chemical and photochemical stability, high specific surface area, optical transparency, electrochemical activities, high electron communicating features and so on, the II–VI semiconductor ZnO nanostructure presents itself as one of the most promising materials for the fabrication of efficient amperometric sensors. Hitherto, very few reports on the use of ZnO nanostructures for the fabrication of an amperometric sensor have been available in the literature.[19–21] Especially, the use of ZnO nanostructures for the fabrication of an electrochemical hydrazine sensor has not been reported yet in the literature.

Here we present, for the first time, an amperometric sensor based on ZnO nanonails synthesized by a thermal evaporation process, for the effective detection of hydrazine. The fabricated hydrazine sensor showed a high sensitivity of 8.56 μA cm^{-2} μM^{-1} with a response time less than 5 s. It shows a linear range from 0.1 to 1.2 μM with a correlation coefficient of R = 0.999 and a detection limit of 0.2 μM.

Fig. 1(a) and (b) show typical SEM images of the as-grown nanonails and reveal that the nanonails are grown in a very high density. Significantly, it is seen that the nanonails are arranged in such a special fashion that they create a perfect spherical peacock-wing like morphology. It is interesting to see that the diameters of the as-grown nanostructures are not uniform along their lengths, but gradually increase from the top to the bottom. A cone-shaped structure forms, having a hexagonal cap which gives the nanostructures a nail-like morphology. The diameters of the nanonails' bases and tops are about 320 ± 50 nm and 60 ± 10 nm, respectively. The caps are about 250 ± 50 nm in diagonal. The XRD pattern shows that the grown nanostructures are single-crystalline wurtzite hexagonal-phase pure ZnO having a dominant peak of ZnO (0002) at 34.2° (Fig. 1(c)), while the EDS spectrum reveals that the nanostructures are formed by zinc and oxygen only (Fig. 1(d)).

Fig. 2(a) shows low-magnification transmission electron microscopy (TEM) images of the as-grown ZnO nanonails. Because of the high density growth of these structures, it is seen from this image that three or more nanonails are merged with each other. Moreover, the dimensions of the nanonails are in good agreement with the SEM observations, clearly showing that the diameters at the bases and the tops of the nanonails are about 280 nm and 60 nm, respectively while their caps are about 200–300 nm in diagonal with a height of ∼300 nm. The selected area electron diffraction (SAED) pattern of the single nanonail indicated by a white arrow (inset in (a)), projected along the $[2\bar{1}\,\bar{1}0]$ zone axis, shows that the formed nanostructures are single crystalline, grown along the [0001] direction. The high-resolution TEM (HRTEM)

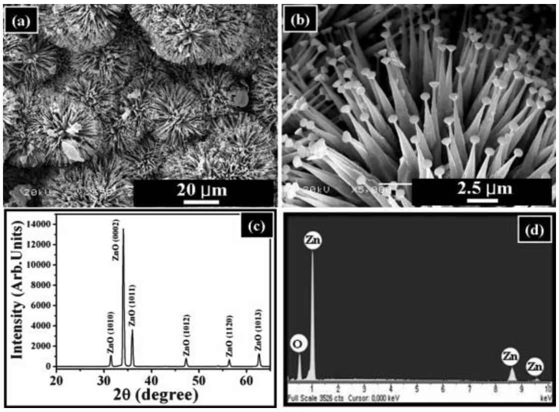

Fig. 1 Low (a) and high (b) magnification SEM images; (c) XRD pattern and (d) EDS spectrum of the as-synthesized ZnO nanonails.

School of Semiconductor and Chemical Engineering and BK21 Centre for Future Energy Materials and Devices, Chonbuk National University, 664-14 Duckjin-Dong 1-Ga, Jeonju 561-756, Republic of Korea.
E-mail: ybhahn@chonbuk.ac.kr; ahmadumar@chonbuk.ac.kr;
Fax: +82-63-270-2306; Tel: +82-63-270-2439

† Electronic supplementary information (ESI) available: Experimental section and ZnO nanorods data. See DOI: 10.1039/b711215g

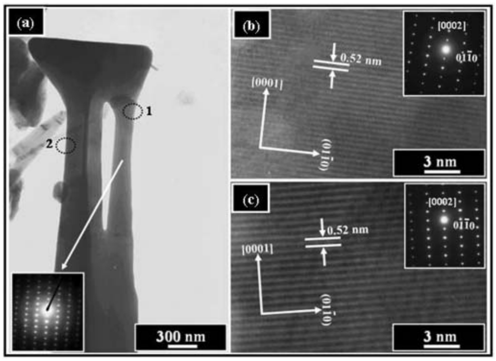

Fig. 2 (a) Low magnification and (b) and (c) high-resolution TEM images of ZnO nanonails indicating the [0001] growth direction with a distance of 0.52 nm between two fringes; insets in (a), (b) and (c) exhibit the SAED pattern images of the corresponding structures indicated with a white arrow and positions (1) and (2) in (a), respectively.

images of the nanonails marked as 1 and 2 in (a) are shown in Fig. 2(b) and (c), respectively. These images show that the distance between two lattice fringes is about 0.52 nm, which corresponds to the *d*-spacing of [0001] crystal planes, consistent with that of the bulk wurtzite crystal of ZnO and confirming that as-grown products are single crystalline with the wurtzite hexagonal phase and grown along the *c*-axis direction. The corresponding SAED patterns of these structures are shown in the insets in Fig. 2(b) and (c), also confirming the consistency with the HRTEM observations.

A strong and dominant peak at 437 cm^{-1} attributed as the Raman active optical-phonon E_2 mode of ZnO crystal, and a very suppressed and small peak at 583 cm^{-1}, assigned to the E_{1L} mode appeared due to the formation of defects such as zinc interstitials and oxygen vacancies, *etc*, have been observed in the Raman-scattering spectrum of ZnO nanonails.[22–24] Furthermore, in the room-temperature PL spectrum, a strong and high intensity peak of UV emission at 381 nm and a suppressed and broad green emission at 521 nm attributed to oxygen vacancy was observed[22] (see ESI†).

Fig. 3(a) shows a cyclic voltammetric sweep curve for the ZnO nanonails-modified gold (Nafion/ZnO/Au) electrode without hydrazine (solid line) and with 1 mM N_2H_4 (dashed line) in 0.01 M phosphate buffer solution (pH = 7.4) at the scan rate of 100 mV s^{-1}. The pH of the solution is important to obtain the efficient electrocatalytic oxidation of hydrazine and it is reported that by increasing the pH value of the solution (pH > 7), the electrocatalytic oxidation of hydrazine increases.[9,25] Therefore, we maintained pH = 7.4 for all the electrochemical experiments. It can be seen that in contrast to the Nafion/ZnO/Au electrode without hydrazine (solid line), a well-defined oxidation peak with 1 mM N_2H_4 in 0.01 M PBS (dashed line) is observed with an E_{pa} (peak potential) of 0.021 V and I_{pa} of 0.905 μA. The oxidation process starts around −0.4 V and the anodic peak appeared at 0.021 V. The electrochemical response is irreversible as no cathodic current is observed during the reverse sweep. According to a previous report,[26] the electrochemical reaction for the hydrazine is proposed to be $N_2H_4 + 5/2OH^- \rightarrow 1/2N_3^- + 1/2NH_3 + 5/2H_2O + 2e^-$. As faster electron transfer leads to a sharper and more well-defined peak, the substantial increase in the peak height reflects a faster electron-transfer reaction. Therefore, hydrazine is effectively detected oxidatively with the Nafion/ZnO modified gold electrode.

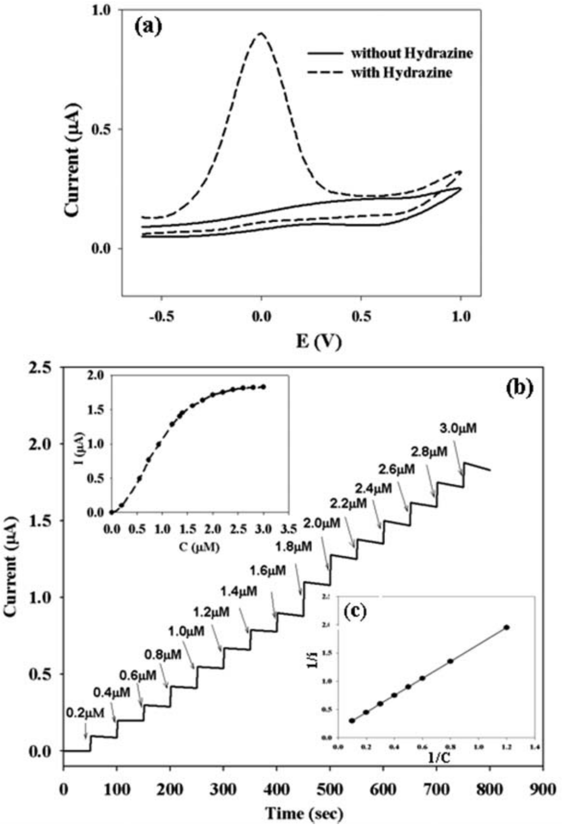

Fig. 3 (a) Cyclic voltammetric sweep curve for the Nafion/ZnO/Au electrode without hydrazine (solid line) and with 1 mM N_2H_4 (dashed line) in 0.01 M PBS (pH = 7.4). The scan rate was 100 mV s^{-1}. (b) Amperometric response of the Nafion/ZnO/Au electrode with successive addition of hydrazine into 0.01 M PBS buffer solution (pH = 7.4). The applied potential was in the range of −0.5 to +0.4 V (*vs.* Ag/AgCl (satd KCl) reference). (c) Plot of 1/*i* *vs.* 1/*C* exhibiting a linear relationship for the steady state current and hydrazine concentration.

Fig. 3(b) shows a typical amperometric response of the Nafion/ZnO/Au electrode on the successive addition of hydrazine (from 0.2–3 μM) into continuously stirred 0.01 M PBS solution (pH = 7.4) at an applied potential in the range of −0.5 to 0.4 V. The amperometric sensor exhibited a rapid and sensitive response to the change of hydrazine concentration and an obvious increase in the oxidation current upon successive addition of hydrazine was obtained. The modified electrode achieved 95% steady-state currents within 5 s. This indicates a good electrocatalytic oxidative and fast electron exchange behaviour of the ZnO nanonails modified electrode. An inset in Fig. 3(b) shows the corresponding calibration curve of the fabricated amperometric hydrazine sensor. The response current increases as the concentration of hydrazine increases, and is saturated at a high hydrazine concentration value near 2.6 μM. Under the optimized conditions, the steady-state current showed a linear relationship with the hydrazine concentration in the range of 0.1 to 1.2 μM (Fig. 3(c)). The correlation coefficient (*R*) was estimated to be 0.999. The sensitivity of the ZnO modified amperometric hydrazine sensor was found, from the slope of the calibration curve, to be 8.56 μA cm^{-2} μM^{-1} and the detection limit was estimated, based on signal to noise ratio

Table 1 Comparison of performances of amperometric hydrazine sensors based on different modified electrode materials

Electrode materials	Sensitivity/ μA cm^{-2} μM^{-1}	Detection limit/μM	Response time/s	Linear range/μM	Ref.
ZnO nanonails	8.56	0.2	< 5	0.1–1.2	This work
ZnO nanorods	4.76	2.2	< 10	0.2–2.0	30
GCE electrode modified with electrodeposited film derived from caffeic acid	3.16	0.4	—	5.0–300	6
Hematoxylin multi-wall carbon nanotubes	0.0208	0.68	< 2	2.0–122.8	16
Carbon nanotubes powder microelectrode	0.9944	—	< 3	—	17
o-aminophenol grafted GCE	0.016	0.5	—	2.0–20.0	27
Manganese hexacyanoferrate modified graphite–wax composite	0.0475	6.65	< 4	33.3–8180	29

(S/N), to be 0.2 μM. The sensitivity of the ZnO modified hydrazine sensors is significantly higher than those of other previously reported amperometric hydrazine sensors based on multi-wall carbon nanotubes modified electrodes,[16] *o*-amino-phenol grafted GCE electrode,[27] multilayer film containing cobalt phthalocyanine,[28] *etc*. The detection limit of the fabricated sensor is also less than those of previously reported hydrazine amperometric sensors.[16,25,27,29] Moreover, it can be considered that the performances of the fabricated sensors also depend upon the morphologies of the ZnO nanostructures. Thus, to check the morphology effect on the performance of the hydrazine sensors, an amperometric sensor based on perfectly hexagonal-shaped ZnO nanorods, synthesized by a thermal evaporation process,[30] was fabricated. The fabricated nanorods based hydrazine sensor showed a sensitivity of 4.76 μA cm^{-2} μM^{-1} with a response time less than 10 s. It showed a linear range from 0.2 to 2.0 μM with a correlation coefficient of R = 0.9914 and a detection limit of 2.2 μM (ESI†). Therefore, one can conclude that the ZnO nanonails are a good candidate, compared to hexagonal-shaped ZnO nanorods, for the fabrication of efficient and highly sensitive hydrazine sensors. In addition to this, for comparing the characteristics and performances of the fabricated ZnO nanonail based hydrazine sensors, the properties of the previously reported hydrazine sensors based on the utilization of different materials as the working electrode are summarized in Table 1.

The stability and reproducibility of the ZnO nanonail modified electrodes for the determination of hydrazine were observed and it was found that the fabricated sensor was stable over more than 45 days in continuous use, with storage in an appropriate form when not in use.

In summary, we have successfully fabricated, for the first time, an electrochemical hydrazine sensor based on ZnO nanonails synthesized by a non-catalytic simple thermal evaporation process. The fabricated hydrazine sensor showed a high and reproducible sensitivity of 8.56 μA cm^{-2} μM^{-1} with a response time less than 5 s and a detection limit of 0.2 μM. The ZnO has multifarious properties such as high specific surface area, nontoxicity, chemical stability, electrochemical activities, and high conductivity which provide high electron communication features that enhance direct electron transfer. The ease of synthesis and electrode fabrication, high sensitivity, low detection limit, and fast response give an opportunity to ZnO nanonails to present themselves as one of the promising nanostructures for the fabrication of efficient amperometric sensors for the detection of hydrazine.

This work was supported in part by the Korea Science and Engineering Foundation grant (R01-2006-000-11306-0) funded by the Korean Government (MOST) and by the Korea Research Foundation grant (KRF-2005-005-J07502) (MOEHRD). KBSI, Jeonju is also acknowledged.

Notes and references

1 S. D. Zelnick, D. R. Mattie and P. C. Stepaniak, *Aviat. Space Environ. Med.*, 2003, **74**, 1285.
2 S. Garrod, M. E. Bollard, A. W. Nicholls, S. C. Connor, J. Connelly, J. K. Nicholson and E. Holmes, *Chem. Res. Toxicol.*, 2005, **18**, 115.
3 S. S. Narayanan and F. Scholz, *Electroanalysis*, 1999, **11**, 465.
4 American Conference of Governmental Industrial Hygenists, *Documentation of Threshold Limit Values and Biological Exposure Indices*, ACGIH, Cincinnati, OH, 1999.
5 E. H. Vernot, J. D. MacEwen, R. H. Bruner, C. C. Haus and E. R. Kinkead, *Fundam. Appl. Toxicol.*, 1985, **5**, 1050.
6 S. M. Golabi and H. R. Zare, *J. Electroanal. Chem.*, 1999, **465**, 168.
7 X. Li, S. Zhang and C. Sun, *J. Electroanal. Chem.*, 2003, **553**, 139.
8 B. Wang and X. Cao, *J. Electroanal. Chem.*, 1991, **309**, 147.
9 S. V. Guerra, C. R. Xavier, S. Nakagaki and L. T. Kubota, *Electroanalysis*, 1998, **10**, 462.
10 S. S. Narayanan and F. Scholz, *Electroanalysis*, 1999, **11**, 465.
11 W. Hou and E. Wang, *Anal. Chim. Acta*, 1992, **257**, 275.
12 I. G. Casella, M. R. Guascito, A. M. Salvi and E. Desimoni, *Anal. Chim. Acta*, 1997, **354**, 333.
13 M. Revenga-Parra, E. Lorenzo and F. Pariente, *Sens. Actuators, B*, 2005, **107**, 678.
14 H. Xia and H.-L. Li, *J. Electroanal. Chem.*, 1997, **430**, 183.
15 H. R. Zare and A. M. Habibirad, *J. Solid State Electrochem.*, 2006, **10**, 348.
16 H. R. Zare and N. Nasirrizadeh, *Electrochim. Acta*, 2007, **52**, 4153.
17 Y. D. Zhao, W. D. Zhang, H. Chen and Q. M. Luo, *Talanta*, 2002, **58**, 529.
18 Y. Lin, F. Lu, Y. Tu and Z. Ren, *Nano Lett.*, 2004, **4**, 191; K. Mukhopadhyay, S. Phadtare, V. P. Vinod, A. Kumar, M. Rao, R. V. Chaudhari and M. Sastry, *Langmuir*, 2003, **19**, 3858; B. R. Azamian, J. J. Davis, K. S. Coleman, C. B. Bagshaw and M. L. H. Green, *J. Am. Chem. Soc.*, 2002, **124**, 12664.
19 F. F. Zhang, X. L. Wang, S. Y. Ai, Z. D. Sun, Q. Wan, Z. Q. Zhu, Y. Z. Xian, L. T. Jin and K. Yamamoto, *Anal. Chim. Acta*, 2004, **519**, 155.
20 Y. F. Li, Z. M. Liu, Y. L. Liu, Y. H. Yang, G. L. Shen and R. Q. Yu, *Anal. Biochem.*, 2006, **349**, 33.
21 A. Wei, X. W. Sun, J. X. Wang, Y. Lei, X. P. Cai, C. M. Li, Z. L. Dong and W. Huang, *Appl. Phys. Lett.*, 2006, **89**, 123902.
22 A. Umar and Y. B. Hahn, *Appl. Phys. Lett.*, 2006, **88**, 173120.
23 A. Umar and Y. B. Hahn, *Nanotechnology*, 2006, **17**, 2174.
24 Y. H. Yang, C. X. Wang, B. Wang, Z. Y. Li, J. Chen, D. H. Chen, N. S. Xu, G. W. Yang and J. B. Xu, *Appl. Phys. Lett.*, 2005, **87**, 183109.
25 E. F. Perez, G. O. Neto, A. A. Tanaka and L. T. Kubota, *Electroanalysis*, 1998, **10**, 112.
26 J. Xu, M. C. Granger and J. Wang, *Proc. Electrochem. Soc.*, 1999, **99**, 403.
27 H. M. Nassef, A. E. Radi and C. K. O'Sullivan, *J. Electroanal. Chem.*, 2006, **592**, 139.
28 C. Sun, Y. Sun, X. Zhang, X. Zhang, D. Jian, Q. Gao, H. Xu and J. Shen, *Thin Solid Films*, 1996, **288**, 291.
29 D. Jayasri and S. S. Narayanan, *J. Hazard. Mater.*, 2007, **144**, 348.
30 A. Umar, S. H. Kim, J. H. Kim and Y. B. Hahn, *J. Nanosci. Nanotechnol.*, 2007, **7**, DOI: 10.1166/jnn.2007.858.